Voltage Dependence of Slow Inactivation in *Shaker* Potassium Channels Results from Changes in Relative K^+ and Na^+ Permeabilities

John G. Starkus,* Stefan H. Heinemann,§ and Martin D. Rayner*‡

From the *Békésy Laboratory of Neurobiology and ‡School of Medicine, University of Hawaii, Honolulu, Hawaii 96822; and §Research Unit Molecular and Cellular Biophysics, Medical Faculty of the Friedrich-Schiller University Jena, D-07747 Jena, Germany

abstract Time constants of slow inactivation were investigated in NH_2-terminal deleted *Shaker* potassium channels using macro-patch recordings from *Xenopus* oocytes. Slow inactivation is voltage insensitive in physiological solutions or in simple experimental solutions such as K^+_o//K^+_i or Na^+_o//K^+_i. However, when $[Na^+]_i$ is increased while $[K^+]_i$ is reduced, voltage sensitivity appears in the slow inactivation rates at positive potentials. In such solutions, the I-V curves show a region of negative slope conductance between ~0 and +60 mV, with strongly increased outward current at more positive voltages, yielding an N-shaped curvature. These changes in peak outward currents are associated with marked changes in the dominant slow inactivation time constant from ~1.5 s at potentials less than approximately +60 mV to ~30 ms at more than +150 mV. Since slow inactivation in *Shaker* channels is extremely sensitive to the concentrations and species of permeant ions, more rapid entry into slow inactivated state(s) might indicate decreased K^+ permeation and increased Na^+ permeation at positive potentials. However, the N-shaped I-V curve becomes fully developed before the onset of significant slow inactivation, indicating that this N-shaped I-V does not arise from permeability changes associated with entry into slow inactivated states. Thus, changes in the relative contributions of K^+ and Na^+ ions to outward currents could arise either: (a) from depletions of $[K^+]_i$ sufficient to permit increased Na^+ permeation, or (b) from voltage-dependent changes in K^+ and Na^+ permeabilities. Our results rule out the first of these mechanisms. Furthermore, effects of changing $[K^+]_i$ and $[K^+]_o$ on ramp I-V waveforms suggest that applied potential directly affects relative permeation by K^+ and Na^+ ions. Therefore, we conclude that the voltage sensitivity of slow inactivation rates arises indirectly as a result of voltage-dependent changes in the ion occupancy of these channels, and demonstrate that simple barrier models can predict such voltage-dependent changes in relative permeabilities.

key words: *Xenopus* oocyte • patch clamp • selectivity • voltage ramp • reversal potential

INTRODUCTION

Inactivation mechanisms of *Shaker* potassium channels have been divided into fast (N-type) and slower (C-type) components (Hoshi et al., 1991). The N-type fast inactivation can be removed by deletion of an NH_2-terminal domain (Iverson and Rudy, 1990; Hoshi et al., 1990). This domain has since been shown to form a tethered inactivation ball that binds to a site within the inner mouth of the permeation pathway (Hoshi et al., 1990; Zagotta et al., 1990). By contrast, slow or C-type inactivation has been shown to produce a constriction of the outer mouth of the permeation channel (Yellen et al., 1994; Liu et al., 1996; Schlief et al., 1996), to involve cooperative interactions between monomers (Ogielska et al., 1995; Panyi et al., 1995), and to develop at a rate that is voltage independent (Hoshi et al., 1991) but markedly affected by both external (López-Barneo et al., 1993; Levy and Deutsch, 1996) and internal (Starkus et al., 1997) monovalent cation concentrations.

Monovalent cations appear to achieve their modulation of inactivation rates by binding to a site within the selectivity filter (Kiss and Korn, 1998) that can be loaded either directly from the external medium or from the internal medium when outward currents are passed (see Starkus et al., 1997). Furthermore, NH_2 terminus–deleted *Shaker* potassium channels are permeable to Na^+ and Li^+ ions when examined using K^+-free, Na^+-substituted, intracellular media (compare Korn and Ikeda, 1995). The Na^+ permeability of noninactivated *Shaker* channels becomes approximately halved as they enter C-type inactivated states (Starkus et al., 1997). By contrast, K^+ permeation is reduced by >100-fold in C-type inactivated *Shaker* channels. These findings suggested that the physiological mechanism of slow inactivation in *Shaker* channels involves marked changes in channel selectivity rather than a complete collapse of the outer region of the permeation pathway. This conclusion has since been supported by Basso et al. (1998), who noted that the permeation path can be

Portions of this work were previously published in abstract form (Rayner, M.D., J.G. Starkus, and S.H. Heinemann. 1999. *Biophys. J.* 76:A412).

Address correspondence to Martin D. Rayner, Director, Békésy Laboratory of Neurobiology, 1993 East-West Rd., University of Hawaii, Honolulu, HI 96822-2359. Fax: 808-956-6984; E-mail: martin@pbrc.hawaii.edu

loaded with Ba^{2+} ions from the external side, even after induction of steady state C-type inactivation.

Chandler and Meves (1965) and Bezanilla and Armstrong (1972) noted that increasing $[Na^+]_i$ produced a voltage-dependent block of outward currents through the delayed rectifier channels of squid giant axons. Subsequently, French and Wells (1977) found that outward currents increased again at very positive potentials, beyond the range that had previously been studied. They found I-V curves to be N shaped, with a region of negative slope conductance between approximately +50 and +150 mV and increasing outward currents at more positive potentials. They suggested that P_K/P_{Na} ratios might change in a voltage-sensitive manner to permit increased Na^+ permeation at these very positive potentials. However, Begenisich and Cahalan (1980) pointed out that N-shaped I-V curves could result from voltage-dependent Na^+ block, followed by progressive relief of this Na^+ block, yielding increasing outward K^+ currents at the more positive potentials. Begenisich and Cahalan (1980) predicted an N-shaped I-V relationship in high $[Na^+]_i$ solutions, from a three-barrier two-site (3B2S) Eyring barrier model in which no more than 5% of total outward current was contributed by the less-permeant Na^+ ions.

Nevertheless, it is now clear that C-type inactivation becomes markedly faster in experiments where Na^+ replaces K^+ as the primary permeating cation (Starkus et al., 1997). The hypothesis suggested by French and Wells (1977) that the N-shaped I-V curve results from a disproportionate increase in Na^+ permeation at very positive potentials would be further supported if the rate of C-type inactivation also increases at these same potentials. We show here that N-shaped I-V curves and voltage-sensitive slow inactivation rates occur together at positive potentials in fast inactivation-deleted *Shaker* channels when both Na^+ and K^+ ions are present in the internal solution. By contrast, simple I-V curves and voltage-insensitive slow inactivation rates occur when only one of these ions is present in the internal solution.

We conclude that both N-shaped I-V curves and voltage-sensitive slow inactivation rates result from relative increases in Na^+ permeation at positive potentials.

Terminology

Recently, Loots and Isacoff (1998) have used fluorescent probes to examine structural changes associated with the slow inactivation process. When fluorescent probes were attached to cysteine residues introduced at carefully chosen sites, it became apparent that slow inactivation involves two normally sequential conformational changes with differing kinetics. An initial step, the "P-type" conformational change, affects the outer end of the selectivity filter. This step is followed by a slower, less readily reversible, "C-type" transition that changes the conformation of the "tower" region of the KcsA structure determined by Doyle et al. (1998), prolongs the slow inactivated state, and stabilizes the S4 segment in its depolarization-favored position (thus left-shifting the Q-V curve; see Olcese et al., 1997). The present paper will follow the modified terminology used by Loots and Isacoff (1998).

MATERIALS AND METHODS

Channel Expression

Data for this study were obtained using the *Shaker* 29-4 construct (Iverson and Rudy, 1990) but with fast, N-type, inactivation removed by deletion of residues 2-29 (McCormack et al., 1994). This construct has been referred to as *ShΔ* in previous papers (Starkus et al., 1997, 1998). However, the primary sequence of *ShΔ* is identical to that of *Shaker* B from S1 through S6; thus, *Shaker* channels will be used as a generic descriptor where results are presumed applicable to both *ShΔ* and *Shaker* B channels. *Xenopus laevis* oocytes were prepared, injected with mRNA, and incubated at 18°C as previously described (Starkus et al., 1997, 1998).

Electrophysiology

Results reported here were obtained from macropatch recordings (Hamill et al., 1981) in either inside-out or outside-out mode, using EPC-9 patch clamp amplifiers (HEKA Elektronik). Patch pipettes were fabricated from aluminum silicate glass, yielding resistances between 0.5 and 2 MΩ in standard solutions. The Pulse+PulseFit software package (HEKA Elektronik) was used to control data acquisition. All experiments were carried out at room temperature (20–22°C) from holding potentials of −100 or −80 mV. Analysis was performed using PulseFit and PulseTools (HEKA Elektronik) for initial processing of the data, and IgorPro (Wavemetrics) for further analysis and generation of figures. Leak and capacitive transients were either subtracted on-line using a variable −P/n correction (Heinemann et al., 1992), or corrected offline from separately recorded, negatively directed control pulses that were appropriately scaled using PulseTools software. Leak holding potential was typically −120 mV, but was reduced to −80 mV for experiments involving long test pulses to very positive potentials.

Voltage ramps were programmed, and both leak and capacitive currents were subtracted online from the resulting data traces, using Pulse+PulseFit software. Recorded data traces were displayed either against time (as in Figs. 5 A and 6 A) or against ramp potential (as in Figs. 4, 5 B, 6 B, and 7). Since any time displacement of the ramp current trace translates to a voltage displacement in the corresponding I-V plot, accurate delineation of I-V data (including reversal potentials) requires minimization of such errors. For 1-ms ramps, we find that analogue Bessel filters should be set to at least 10 kHz, while the sampling interval should not be >10 μs. Additionally, where nonlinear leak occurs in the control pulses, the entire I-V trace may be offset up- or downwards relative to the zero current axis. Such offsets can also produce substantial errors in E_{rev} measurements. To avoid this problem, leak pulses should be carefully monitored and data should be discarded where excessive leak is noted. (The points noted above can be verified through control experiments using patches exposed to symmetric mono-ionic solutions.)

Additional errors in E_{rev} can arise from changes in ion concentrations associated with the pulse sequences used to make these measurements. Large initial currents can deplete ion concentrations on one side of the membrane while adding ions to the

other side. Such changes may equilibrate within milliseconds or be relatively long lasting, depending on the magnitude and duration of the currents, as well as on the volumes of the diffusion-restricted spaces.

When single patches were exposed to multiple internal or external solutions, solution changes were carried out either (a) by exchange of the entire bath volume, or (b) by positioning the pipette tip in the outlet path of a valve-operated quartz-capillary manifold. Thus, inside-out patches were used to explore effects of internal solutions changes (Fig. 7 A), whereas outside-out patches were used when external solution changes were required (Fig. 7 B).

Solutions

In addition to monovalent chloride counter ions, all external solutions contained 1.8 mM Ca^{2+} and 10 mM HEPES, adjusted to pH 7.2. Internal solutions contained 1.8 mM EGTA and 10 mM HEPES, adjusted to pH 7.2. External solutions used here contained (mM): NFR: 2.5 KCl, 115 NaCl; Na-Ringer: 115 NaCl; K-Ringer: 115 KCl; Tris-Ringer: 115 TrisCl. Internal solutions contained (mM): K-EGTA: 115 KCl; Na-EGTA: 115 NaCl; Tris-EGTA: 115 TrisCl. Appropriate complex solutions were created, as needed, by appropriate mixing of these stock solutions. In the figures, solutions are specified by the concentrations (mM) of monovalent cations: external//internal. Thus, solutions denoted as 115 Na^+_o//115 K^+_i, involve Na-Ringer as the external solution and K-EGTA as the internal solution, etc.

Data Analysis and Modeling

Double-exponential analysis of tail current time courses (see Fig. 2) was carried out by fitting ionic current traces with the following equation:

$$I(t) = a_0 + a_1 \exp(-t/\tau_f) + a_2 \exp(-t/\tau_s), \quad (1)$$

where a_0 is the predicted steady state current, a_1 and a_2 are the zero time intercepts of the first and second exponential components, and τ_f and τ_s are the corresponding time constants for these components. Similarly, time constants for slow inactivation were determined by fitting a single exponential version of this equation to the dominant time constant of the inactivation process.

Ion permeation through a channel described by a one-site two-barrier Eyring model was calculated using a common-domain software program downloaded as described in Nonner et al. (1998) and by routines written in IgorPro according to the formalism described by Hille (1992). P_K/P_{Na} ratios were calculated from E_{rev} data in various Na^+ and K^+ solution mixtures such as those used in this study. For modeling, we assumed that Ca^{2+} permeability through *Shaker* channels is negligible.

RESULTS

Slow inactivation in *Shaker* potassium channels is less complete at negative potentials than at positive potentials and thus the steady state level of inactivation is voltage dependent. Nevertheless, slow inactivation develops with time constants that appear to be voltage insensitive (Hoshi et al., 1991) under standard experimental conditions. The present paper explores an interesting exception to this general observation and seeks to understand one mechanism by which slow inactivation can develop substantial apparent voltage sensitivity.

Slow Inactivation Appears Voltage Sensitive at Positive Potentials when both Na^+ and K^+ Ions Are Present in the Internal Solution

Three representative families of macroscopic currents, obtained from inside-out macro patches in different experimental solutions are shown in Fig. 1. Fig. 1 A, with 115 mM Na^+_o and 115 mM K^+_i (see materials and methods) shows the voltage-insensitive kinetics characteristic of slow inactivation under relatively physiological conditions. Test pulses were 500 ms in duration and ranged from −60 to +160 mV in 10-mV steps. Interpulse intervals were 5 s in these sequences to minimize cumulative slow inactivation. Similarly, Fig. 1 B presents results from an experiment in which the internal potassium has been replaced by 115 mM Na^+_i. Although the slow inactivation rate is slow in Fig. 1 A and very fast in B, no voltage sensitivity is apparent in either case. By contrast, when 10 mM K^+ is added to the 115 mM internal Na^+ solution (see Fig. 1 C) changes in inactivation rate become readily visible at the more positive test potentials.

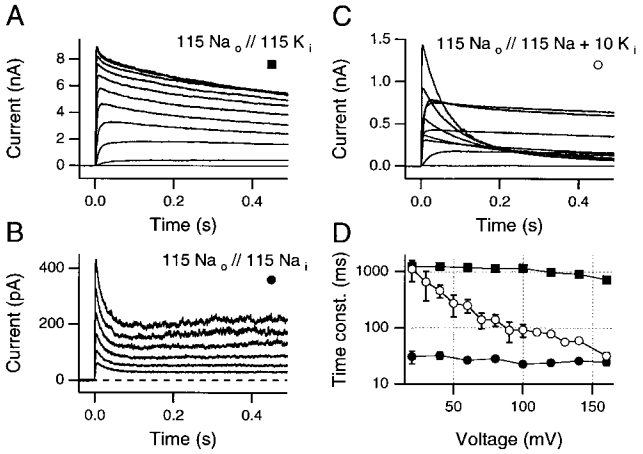

Figure 1. Slow inactivation rates can become steeply voltage sensitive when high Na^+, low K^+, internal solutions are used. (A) With 115 mM [Na^+] externally and 115 mM [K^+] internally, slow inactivation rate is essentially voltage insensitive for test potentials between +20 and +160 mV (traces shown: −20 to +160 mV, 20-mV steps, 5-s interpulse intervals). (B) Despite a marked increase in the rate of slow inactivation in symmetric Na^+ solutions, the slow inactivation rate remains insensitive to the test potential (traces shown: +40 to +140 mV, 20-mV steps, 5-s interpulse intervals). (C) Slow inactivation is steeply voltage sensitive when 10 mM of K^+ is added to the internal solution used in B (traces shown: −60 to +120 mV, 20-mV steps, 5-s interpulse intervals). (D) Time constants for all three conditions for test potentials from +20 to +160 mV. ■, 115 Na_o//115 K_i as in A (mean data from three to five patches). ●, 115 Na_o//115 Na_i as in B (mean data from two to four patches). ○, 115 Na_o//115 Na_i + 10 K_i as in C (mean data from three patches, except at +160 mV, where n = 14 patches). Standard deviations are visible only when they exceed the size of the data symbol. All data are from inside-out patches.

This surprising finding could be readily explained if the outward currents in Fig. 1 C were all carried primarily by K^+ ions, as was indicated by the work of Begenisich and Cahalan (1980). In this case, at test potentials greater than +50 mV, the low (10 mM) internal K^+ concentration could become too depleted during these long (500-ms) pulses to sustain large outward currents. According to this hypothesis, the increasingly rapid apparent inactivation seen at >50 mV would be an artifact of increasing, cumulative $[K^+]_i$ depletion. This hypothesis will be further considered in the next section.

However, López-Barneo et al. (1993) showed that external monovalents slow the inactivation rate as if binding to a regulatory site with the following affinities: $K^+ > Rb^+ >> Na^+ > Cs^+ > NH_4^+$. Furthermore, Starkus et al. (1997) noted that the hypothesized regulatory site can be loaded from the internal solution by outward currents. Thus, an alternative mechanism by which the apparent voltage sensitivity of slow inactivation might be produced is suggested by the results shown in Fig. 1 D. In this panel, the dominant time constant of slow inactivation is plotted against test potential for the three ionic conditions shown in Fig. 1, A–C. Little voltage sensitivity is evident in either Na^+_o / / K^+_i solutions (■) or in Na^+_o / / Na^+_i solutions (●), despite the ~50-fold difference in the inactivation time constants between these two conditions. By contrast, when both Na^+ and K^+ ions were present in the internal solution (○), we see that inactivation time constants near 0 mV are similar to the values of Fig. 1 A, although at more than +150 mV, inactivation time constants approach closely those seen in B. If P_K/P_{Na} changes as a function of potential (as suggested by French and Wells, 1977), then the voltage sensitivity evident in Fig. 1 C could arise from changes in the relative contributions of K^+ and Na^+ ions to the observed outward currents. K^+ ions might carry the outward current at more negative potentials, whereas Na^+ ions could become the primary permeant ion species at very positive potentials.

Apparent Voltage Sensitivity of Slow Inactivation Rates Appears Correlated with Specific Components of the N-Shaped I-V Waveform

The results presented in Fig. 1 suggest that the apparent voltage sensitivity of slow inactivation appears when both Na^+ and K^+ ions are present in the internal solutions. These same conditions have previously been found to produce the N-shaped I-V waveform (French and Wells, 1977; Begenisich and Cahalan, 1980). However, any more detailed correspondence is difficult to evaluate from the superimposed family of traces shown in Fig. 1 C. Therefore, Fig. 2 A divides data traces from the same patch into four panels (a–d). These panels

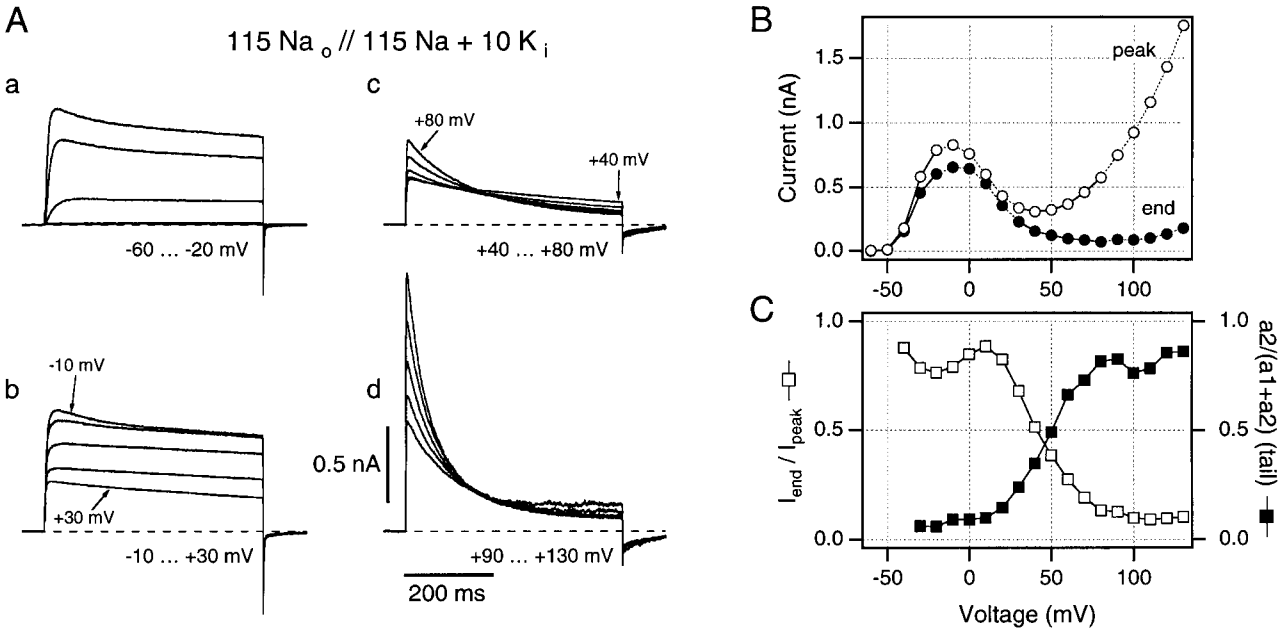

Figure 2. A family of macropatch currents recorded from *ShΔ* channels expressed in *Xenopus* oocytes, using a high [Na^+], low [K^+] internal solution. (A, a–d) Individual current traces are shown for groups of five test potentials to minimize the ambiguity produced by overlapping traces. (B) Peak current magnitudes (○) give an N-shaped peak I-V curve, while end currents (●) fail to increase at potentials greater than +20 mV, indicating steadily increasing slow inactivation in this 500-ms time window at these test potentials. (C) I_{end}/I_{peak} (□) and the relative increase in magnitude of slow component of the tail current (■) are plotted against the test potential to give quantitative estimates of steady state slow inactivation at these potentials. Symbols in B and C are connected by straight lines. All data are from the same inside-out patch as in Fig. 1 C. Traces recorded using 5-s interpulse intervals.

show the currents corresponding to the regions of differing slope in the N-shaped I-V curve (Fig. 2 B).

In Fig. 2 A, a, outward currents are shown for step depolarizations from holding potential to test potentials between −60 and −20 mV. These currents show typical features of outward K^+ currents through *Shaker* channels: activation is steeply voltage sensitive, and slow inactivation becomes apparent in the −20- and −30-mV traces. Currents in Fig. 2 A, b, correspond to the region of negative slope conductance in the I-V curves (Fig. 2 B, −10 to +30 mV). Thus, peak outward current is largest at −10-mV test potential, with the smallest peak current being at +30 mV. In this voltage range, tail current peaks decrease in linear relation to the end-of-trace currents, and slow inactivation rates appear similar to those in Fig. 2 A, a. In Fig. 2 A, c, currents are relatively small and correspond to the "saddle" region of the I-V curves (Fig. 2 B, +40 to +80 mV). However, in this region of the I-V curve, changes in the kinetics of slow inactivation are directly visible in the data traces. Over this range of potentials, the dominant slow inactivation time constant changes from ~500 ms at +40 mV to ~160 ms at +80 mV. Furthermore, the fast tail current peak noticeable in Fig. 2 A, a and b, is markedly reduced and a slow component becomes more readily visible (see Fig. 2 C, ■). Currents in Fig. 2 A, d, cover the range from +90- to +130-mV test potential. The peak current increases steeply with test potential, while the inactivation time constant falls from 150 to 55 ms between +90 and +130 mV. The most obvious voltage sensitivity of slow inactivation rates appears at more than +50 mV, while an apparent maximum rate is approached as outward currents increase at positive potentials (see Fig. 1 D).

Fig. 2 C provides two measures of the extent to which slow inactivation occurs during the isochronal (500-ms) pulses shown here. Open symbols show the ratio of the peak currents to the end-of-trace currents from the Fig. 2 B I-V curves and report the fraction of noninactivated channels at the end of the test pulse. Closed symbols were obtained from double-exponential analysis of the tail currents from Fig. 2 A (see Eq. 1), and show the ratio $a_2/(a_1+a_2)$ where a_1 and a_2 are the weighting factors for the fast and slow kinetic components (τ_f and τ_s, respectively) in these tail currents. As shown by Starkus et al. (1997, 1998), this ratio indicates the fraction of channels that enter the slow-inactivated state during these pulses. Both approaches are consistent in suggesting that the amount of inactivation that occurs within this 500-ms window increases substantially towards the end of the negative slope region of the N-shaped I-V curve and saturates at very positive potentials.

It seems clear that the negative slope conductance section of the I-V curve, corresponding to increased voltage-dependent Na^+ block of outward K^+ currents (Chandler and Meves, 1965; Bezanilla and Armstrong, 1972), coincides with the voltage range where inactivation rate also begins to increase (compare Figs. 1 D and 2, B and C). Furthermore, inactivation rates continue to increase through the saddle region of the I-V curve, approaching rates equivalent to those in pure Na^+_i solutions (see above) at around +150 mV. However, this correspondence in rates at very positive potentials might be purely coincidental, if the rapid inactivation seen at positive potentials is an artifact of $[K^+]_i$ depletion.

Although test pulse $[K^+]_i$ depletion should be correlated with current magnitude, Fig. 2 A, c, shows that inactivation rates start to increase in the saddle region of the N-shaped I-V curve, well before peak currents again reach the ~1-nA levels seen at around −20 mV (see Fig. 2 A, a and b). Thus, if inactivation is getting faster although currents are still smaller than at their −20-mV level, then internal K^+ depletion arising during each individual test pulse cannot explain these changes in inactivation rate. However, cumulative K^+ depletion might occur as a result of the preceding sequence of ~1-nA currents, despite the 5-s interpulse intervals used here. Depletion that lasts 5 s or more suggests a larger diffusion-restricted space than seems likely to be present on the continuously perfused internal surface of an inside-out patch. Nevertheless, assuming that this might be the case, the cumulative depletion hypothesis was tested by reversing the pulse order (i.e., starting with a first pulse to +140 mV and working back to less positive potentials). No detectable hysteresis occurred in the N-shaped I-V curve, and essentially identical inactivation rates were obtained at positive potentials using this reversed pulse sequence. We conclude that neither pulse-specific nor cumulative depletion of $[K^+]_i$ can be the direct cause of the rapid inactivation seen at potentials greater than +50 mV.

Thus, while it was appropriate that Begenisich and Cahalan (1980) should assume that the Na^+ block of outward K^+ currents was relieved by increased K^+ permeation at these positive potentials, the inactivation rates observed here suggest a different hypothesis. Specifically, Na^+ permeation increases while K^+ permeation decreases at positive potentials. We describe next a series of indirect tests for this hypothesis.

If the apparent voltage sensitivity of slow inactivation in Fig. 1 C arises from voltage-dependent changes in P_K/P_{Na}, then voltage sensitivity should not appear when either K^+ or Na^+ is the only cation present in the internal solution. Inactivation time constants change from ~5 s in symmetric 115 mM K^+ solutions to ~50 ms in symmetric Na^+ solutions. However, the voltage sensitivities of the time constants remain closely similar when evaluated using linear regression of ln τ (milliseconds) against V_{test} (between 0 and approximately +130 mV). Mean slope for solutions containing 115 Na^+_o//115 Na^+_i; 115 K^+_o//115 K^+_i; 115 Na^+_o//115 K^+_i; 115

$Tris^+_o$//115 Na^+_i; and 115 $Tris^+_o$ + 2.5 Na^+_o//115 K^+_i was -0.0016 ± 0.0064 mV^{-1} ($n = 15$ experiments). This slope is not significantly different from zero, indicating that slow inactivation remains voltage insensitive, even at very positive potentials in these simple solutions. Nevertheless, the time constant seen in Na^+_o// Na^+_i solutions at +160 mV (31.1 ± 2.9 ms, $n = 3$) is significantly slower than in $Tris^+_o$//Na^+_i at the same potential (4.4 ± 1.3 ms, $n = 3$), suggesting that external Na^+ ions make an additional contribution to loading of the regulatory site.

If the apparent voltage sensitivity of slow inactivation arises from voltage-sensitive changes in P_K/P_{Na}, then inactivation will appear voltage sensitive when internal solutions contain significant quantities of both Na^+ and K^+ ions. To evaluate this prediction, internal solutions containing 10 mM K^+_i plus either 115 Na^+_i or 58 mM Na^+_i (Tris substituted) were used, yielding the general result that all "mixed" internal solutions (containing both Na^+ and K^+ ions) produced voltage-sensitive inactivation rates. However, small but significant differences were noted as a result of the external solutions used. These were either "simple" (115 mM Na^+_o or $Tris^+_o$) or mixed (containing Na^+_o or $Tris^+_o$, plus 2.5–10 mM of added K^+_o). The mean slope for simple external solutions was -0.0200 ± 0.0034 mV^{-1} ($n = 7$), which is equivalent to −50 mV per e-fold change. However, for mixed external solutions, the mean slope increased to -0.0303 ± 0.0029 mV^{-1} ($n = 9$), which is equivalent to −33 mV per e-fold change. By unpaired, two-tailed t test, both slopes were significantly different from zero ($P < 0.0001$). Furthermore, the difference between the slopes obtained in the presence and absence of mixed external solutions was also extremely significant ($P < 0.0001$). These findings support the hypothesis that P_K/P_{Na} changes as a function of voltage, although the additional effect of mixed $Na^+ + K^+$ external solutions suggests a continuing regulatory effect of external ion concentrations even during outward currents.

If *Shaker* channels permit Na^+ ions to permeate more readily than K^+ ions at very positive potentials, then inactivation rates seen at +160 mV should be relatively insensitive to the addition of internal K^+ ions. When the time constant in Na^+_o//Na^+_i (31.1 ± 2.9 ms, $n = 3$,) is compared with that seen in Na^+_o//Na^+_i + 10 mM K^+_i (31.7 ± 18.9 ms, $n = 14$), no significant effect of internal K^+ is noted. Similarly, this lack of effect of internal K^+ persists at very positive potentials, even when Na^+_i is reduced first to 58 mM (31.0 ± 6.8 ms, $n = 3$), and then to 29 mM (30.8 ± 3.1 ms, $n = 2$). Apparently, adding 10 mM K^+_i does not permit internal K^+ ions to reach the regulatory site to any significant extent at +160 mV, when as little as 29 mM Na^+ is present in the internal solution. Given previous conclusions that the regulatory site lies within the permeation path (Kiss and Korn, 1998), it seems unlikely that the outward currents observed at these potentials can be carried by K^+ ions.

Although the evidence presented above is indirect, this substantial series of observations suggests that the apparent voltage sensitivity of slow inactivation arises from changes in relative permeabilities for Na^+ versus K^+ ions, such that Na^+ ions become increasingly likely to permeate *Shaker* channels at positive potentials and displace K^+ ions from the inactivation-regulating site. We provide below additional evidence to support the concept that Na^+ ions can permeate *Shaker* channels at very positive potentials, while also addressing the mechanisms that might underlie such voltage sensitive changes in P_K/P_{Na}.

Although our first test of the $[K^+]_i$ depletion hypothesis (see above) shows that $[K^+]_i$ depletion is not the cause of the changes in slow inactivation rates seen here, it is clear that $[K^+]_i$ depletion permits Na^+ permeation even at negative potentials in some potassium channels (Korn and Ikeda, 1995; Starkus et al., 1997). Thus, rapid depletion of $[K^+]_i$ during pulses to very positive potentials would increase Na^+ permeation and increase inactivation rate, providing an interesting possible mechanism that could explain our results. Alternatively, rapid slow inactivation might be producing changes in P_K/P_{Na}, as reported by Starkus et al. (1997, 1998). Finally, steps to very positive potentials might result in either state-dependent change of channel selectivity equivalent to the effect observed by Immke et al. (1999) or more direct effects of voltage on the parameters that determine the selectivity of *Shaker* channels (see discussion).

Outward Na^+ Currents Increase Nonlinearly at Positive Potentials

To conclude that Na^+ permeation increases at positive potentials would require either that $[K^+]_i$ becomes rapidly depleted, or that *Shaker* channels are capable of passing significant outward Na^+ currents at these potentials in the presence of internal K^+ ions, despite the previously described block of Na^+ tail currents by internal K^+ ions at negative potentials (Korn and Ikeda, 1995; Starkus et al., 1997; Ogielska and Aldrich, 1998). As a first step, we explored these concepts by comparing the voltage sensitivity of outward currents in the absence (Fig. 3 A) and presence (B) of 10 mM internal K^+.

For the solutions used in Fig. 3 A, all outward currents must be carried by Na^+ ions. Small inward currents are seen at negative potentials. However, at test potentials larger than +80 mV, outward Na^+ current increases in a markedly nonlinear manner, reaching >2 nA at +140 mV. Clearly, large outward Na^+ currents can occur at test potentials larger than +100 mV. Even after slow inactivation, the steady state outward Na^+

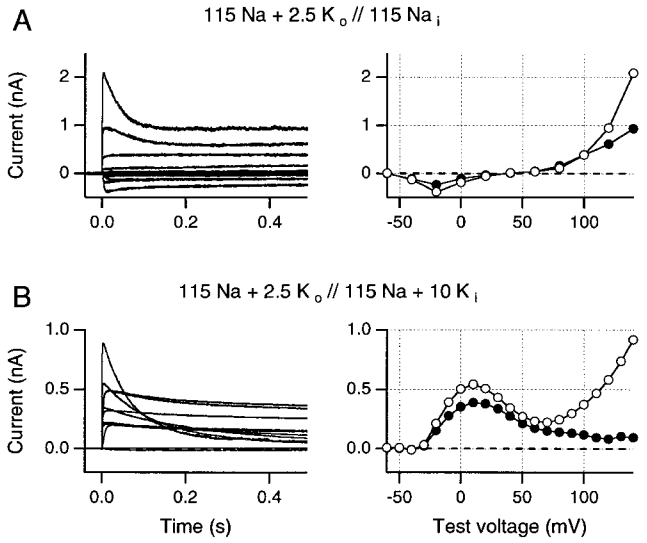

Figure 3. Current families were obtained using a K^+-free internal Na^+ solution (A) and, in a different patch, following addition of 10 mM internal K^+ (B). Holding potential was −80 mV and currents were recorded using on-line −P/n protocols for leak and capacity current subtraction. Test pulse voltages increased by 20-mV increments in A and by 10-mV increments in B. (A) In the absence of internal K^+ ions, all outward currents are carried by Na^+ ions. Both peak Na^+ currents (○) and steady state outward Na^+ currents (●) increase steeply at potentials greater than +80 mV. Inactivation becomes readily apparent only at the most positive potentials. (B) In the presence of internal K^+ ions, peak currents (○) increase to a maximum at +10 mV, followed by a region of negative slope conductance between +20 and +70 mV. At potentials greater than +80 mV, peak currents rise steeply again, just as in A. However, end currents fall steadily at potentials greater than +10 mV (●). Symbols are connected by straight lines. Data in A and B were obtained from two different inside-out patches. All traces recorded using 5-s interpulse intervals.

current remains ~1 nA at +140 mV (●); that is, at 43% of peak current magnitude. Slow inactivation in this +140-mV trace was well fitted by a single time constant of 37.5 ms, which seems reasonably comparable to the mean time constant of 31.1 ± 2.9 ms seen at +160 mV (see above).

In Fig. 3 B (from a different patch), we show the effect of adding 10 mM internal K^+, while retaining 2.5 mM external K^+. The reversal potential is here approximately −35 mV, indicating that P_K/P_{Na} is ~400 and, hence, that Na^+ permeation must be negligible at negative potentials, as shown in previous studies. The peak outward current maximum for the N-shaped I-V curve is shifted from −10 mV in Fig. 2 B to +10 mV in Fig. 3 B, with a zone of negative slope conductance between +10 and +60 mV leading to steeply increasing outward currents at more positive potentials. These outward currents increase in the same potential range as the outward Na^+ currents seen in Fig. 3 A. Similarly, the slow inactivation time constant is 74 ms at +140 mV in this record, as would be expected if Na^+ was the primary, although not the only, determiner of inactivation rate under these conditions. Note also that the steady state outward current in inactivated channels is markedly suppressed by internal K^+ ions, falling to 11% of peak current after 500 ms at +140 mV.

Fast Voltage Ramps Can Be Used for Evaluation of "Instantaneous" I-V Curves

In contrast to the indirect evidence offered above, relatively direct evidence as to the nature of the ions permeating at different potentials should be obtainable from comparisons of instantaneous I-V curves from the same patch in solutions of different ionic content. Unfortunately, the standard tail current method for evaluation of instantaneous I-V curves requires a series of pulses separated by intervals sufficient to permit full recovery from any slow inactivation that may have occurred. A faster method for recording instantaneous I-V curves would permit more complete data sets to be obtained from single patches, before significant channel rundown. We have therefore explored the use of fast (1-ms) voltage ramps for evaluation of instantaneous I-V curves.

Data shown in Fig. 4, A and B, were obtained using both the fast ramp and standard tail current protocols from the same outside-out patch, following 10-ms prepulses to +40 mV. These prepulses were then followed either by a 1-ms descending ramp to a return potential of −100 mV, or by steps to different return potentials (see Fig. 4 A) for conventional instantaneous I-V analysis. Data traces are shown in Fig. 4 A. Fig. 4 B shows the current recorded during the 1-ms ramp (continuous curve) plotted against the ramp potential, thus tracing out an instantaneous I-V plot. Such curves start from the end-of-trace current value reached after 10 ms at test potential (+40 mV), and finish at −100 mV return potential. For comparison, data points from analysis of tail current records (Fig. 4 B, ○) are also shown in these plots. The close correspondence seen here between the two methods suggests that the results obtained using fast ramps can be viewed with reasonable confidence.

The results presented in Fig. 4, C and D, address an equivalent issue: the degree of correspondence between N-shaped I-V curves as seen in fast ramps and the N-shaped I-V curves demonstrated from test-pulse currents (see Figs. 1–3). Data were recorded from an inside-out patch exposed to 115 mM Na^+_o//115 mM Na^+_i + 10 mM K^+_i while using 5-ms test pulses ranging from −60 to +150 mV. As shown in the pulse diagram of Fig. 4 C, each test pulse was followed by a voltage ramp from test potential to −100 mV. Original data traces are shown in Fig. 4 C; in Fig. 4 D, data points (○) obtained from peak currents at test potential are com-

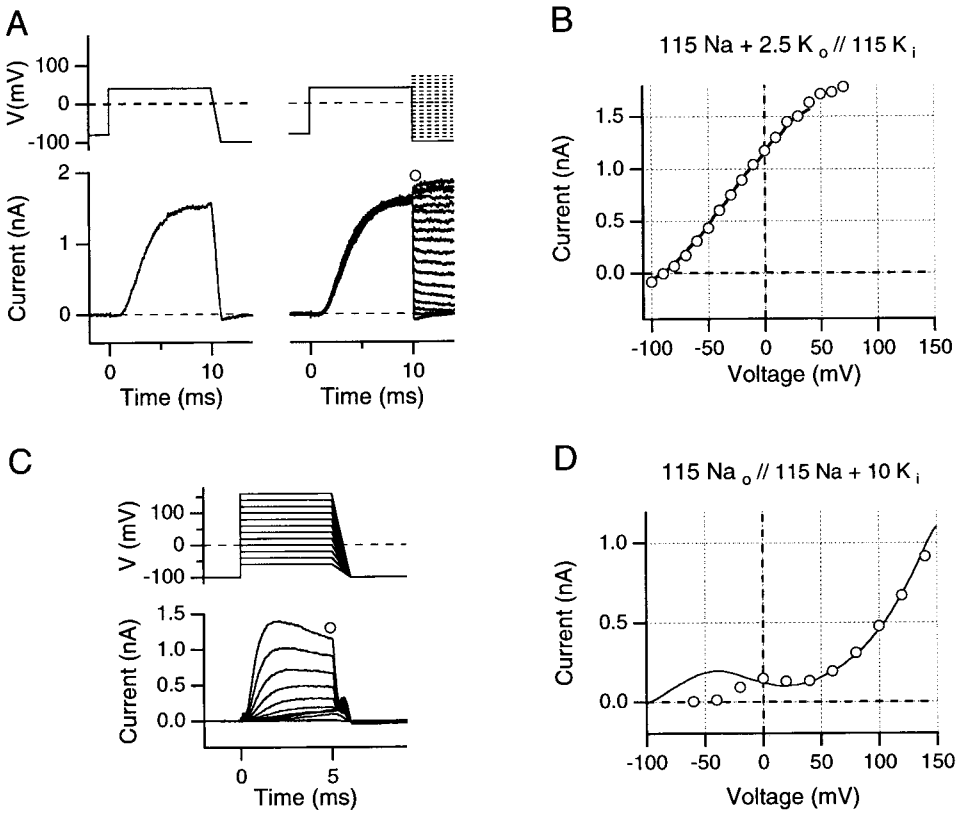

Figure 4. (A and B) Comparison of instantaneous I-V curves and reversal potentials obtained from 1-ms ramps and by the standard tail current method, evaluated in high internal K^+ solution (A, top) The pulse protocols illustrate the 1-ms downward ramps from +40 as well as corresponding protocols for the recording of instantaneous tail currents. (Bottom) Ionic currents obtained from an outside-out patch using solutions indicated in B. Data were recorded with a sample interval of 10 μs, digitally low-pass filtered at 20 kHz. (B) Comparison of ramp I-V data from +40 mV to −100 mV (solid line) with instantaneous tail current I-V data (○) from the data shown in A. (C and D) Comparison of instantaneous I-V curves from 1-ms ramps with the N-shaped test pulse I-V curve, evaluated in a high internal Na^+ solution with 10 mM added K^+. (C, top) The pulse protocols are indicated; note that in low internal K^+ concentration, yielding faster inactivation, short (5-ms) depolarizing pulses were used. All records were leak- and capacitative-current subtracted using on-line −P/n pulses. (Bottom) Ionic currents obtained from an inside-out patch using the solutions indicated in D. (D) Comparison of ramp I-V data from +160 to −100 mV (solid line) with test pulse peak current I-V data (○) from the data shown in C. Note the N-shaped I-V curve for both the ramp and the test pulse I-V curves. All data were obtained using 5-s interpulse intervals.

pared with the ramp I-V from the most depolarized voltage step (continuous curve). In both cases, an N-shaped I-V is apparent, and satisfactory correspondence is demonstrated between the results of these methods at positive test potentials. At negative test potentials, the curves necessarily diverge, since test-pulse currents are limited by incomplete channel activation. Thus, a current maximum occurs at 0 mV in the test pulse I-V, but at approximately −40 mV in the ramp I-V.

These results provide additional evidence against $[K^+]_i$ depletion being the mechanism that permits outward Na^+ currents to occur at very positive potentials. That hypothesis requires the persistence of substantial $[K^+]_i$ depletion between positive pulses 5-s apart, so as to bring about cumulative depletion of $[K^+]_i$ during a sequence of 5-ms test pulses. However, as shown in Fig. 4 D, the last pulse in the depolarizing sequence is followed by a downward ramp in which the observed current accurately reproduces the N-shaped I-V curve. If $[K^+]_i$ falls sufficiently during the test-pulse sequence to permit outward Na^+ currents to occur at more than +60 mV, it seems highly improbable that $[K^+]_i$ could recover sufficiently to support outward K^+ currents of approximately normal magnitude at 0 mV during the course of a 1-ms downward ramp from +150 mV. Thus, although it is clear that outward K^+ currents will produce both transitory increases in $[K^+]_o$ and decreases in $[K^+]_i$, these effects are neither large enough nor long lasting enough to be the primary cause of either the N-shaped I-V or its associated changes in slow inactivation rates.

Ramp I-V Curves from Noninactivated and Slow Inactivated Channels

As noted above, the hypothesis that voltage-dependent changes in relative Na^+ and K^+ permeation underlie the N-shaped I-V relationship should be addressable from detailed studies of I-V waveforms after changes in internal and external ion concentrations. However, slow inactivation alters channel selectivity (see Starkus et al., 1997, 1998), and voltage-dependent changes in the rate of slow inactivation must alter the relative fractions of K^+- versus Na^+-conducting channels at different times and at different test potentials, changing the effective P_K/P_{Na} ratio of the membrane patch. Thus,

slow inactivation-induced changes in overall permeation properties provide an alternative mechanism that might underlie the N-shaped I-V curves. We have already demonstrated (see Fig. 4, A and B), that equivalent I-V curves can be obtained using either single 1-ms ramps or the conventional tail-current method. Note also that the 1-ms duration of the ramps used here is short by comparison with the fastest time constants for slow inactivation in internal solutions containing both Na^+ and K^+ ions ($\sim$30 ms, see above).

Effects of prepulse duration on ramp I-V waveforms were studied at two different test potentials, +40 mV (Fig. 5) and +160 mV (Fig. 6). The +40 mV test potential was chosen to represent the low point of the saddle in the N-shaped curve that would correspond, potentially, to the region of maximum Na^+ block. By contrast, at +160 mV, Na^+ block might well have been substantially relieved. Since both data sets were obtained from the same patch, similar quantitative estimates for the peak current at approximately −40 mV would indicate the equivalence of instantaneous conductance curves reached from these potentially dissimilar initial conditions. Furthermore, since slow inactivation rates are also quite different at these two potentials, we reasoned that the extent of this mechanism's involvement in the N-shaped I-V curve would also be readily apparent from such data.

Fig. 5 A (left) shows superimposed data traces for 5-, 15-, and 45-ms test pulses (end-current levels for 165- and 600-ms pulses are indicated by dotted lines on this plot). Fig. 5 A (right) shows the ramp current sections of these traces, superimposed, and on an expanded time base that is aligned with a schematic presentation of the voltage ramp. Fig. 5 B shows the same currents plotted against ramp voltage. It is now clear that the artifact-like "spikes" in Fig. 5 A resulted from the maximum current occurring in the negative region of the ramp I-V curve. Just as in Fig. 4 D, this maximum occurs at approximately −40 mV. Also, Fig. 5 B (left) shows suppression of these maximum currents in approximate proportion to the suppression of the end currents by slow inactivation. Fig. 5 B (right) shows an expanded region of the ramp I-V traces. In the 5- and 15-ms traces, E_{rev} shifts to the right (from −99 to −90 mV), and further right shifting occurs after 45 ms (to −83 mV), 165 ms (to −80 mV), and 600 ms (to −76 mV). Since these shifts do not seem to be proportionate to the small amount of slow inactivation shown from end-current reduction, they may be caused, in part, by extracellular K^+ accumulation. In support of this interpretation, we note that peak tail currents increase (Fig. 5 A) with prepulse duration, rather than decreasing, as would be expected from inactivation alone. Only after the longest prepulses (at +40 mV)

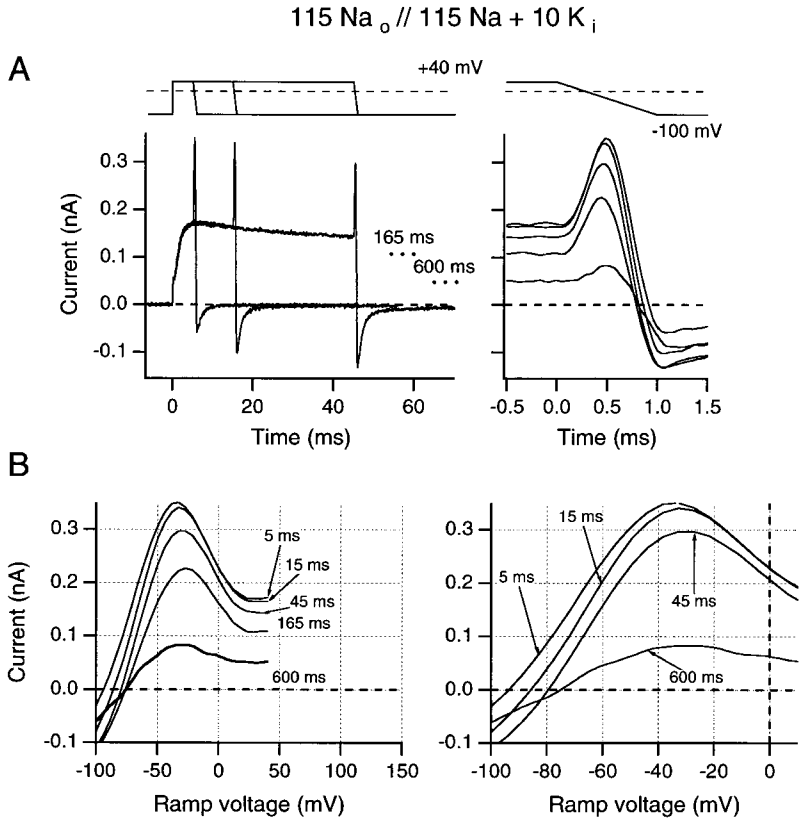

Figure 5. Effects of increasing test pulse duration on ramp I-V curves recorded following test pulses to +40 mV. Ramp currents are plotted against time (A) and against the ramp potential (B). Solutions were identical to those used in Fig. 4 B. (A, left) Superimposed data traces for 5-, 15-, and 45-ms test-pulse durations. End current levels for 165 and 600 ms are indicated by dots. (Right) The same ramp currents superimposed and aligned with the voltage record (top trace). (B, left) Ramp currents after test pulses shown in A are plotted against ramp voltage (from +40 to −100 mV). (Right) An expanded voltage scale is used to illustrate changes in reversal potential. All data were obtained from one inside-out patch using 5-s interpulse intervals.

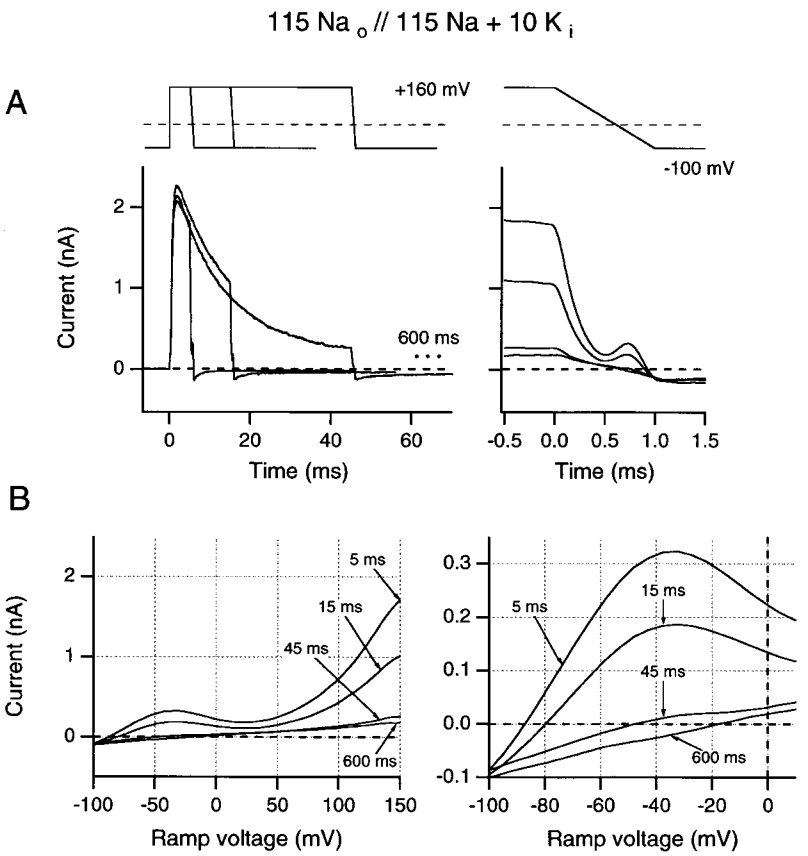

Figure 6. Effects of increasing test pulse duration on ramp I-V curves recorded after test pulses to +160 mV. (A) Ramp currents are plotted against time. (B) Ramp currents are plotted against ramp potential. Same format as in Fig. 5. All data are from the same inside-out patch as in Fig. 5.

will E_{rev} be substantially affected by the accumulation of slow inactivated channels. This issue is further addressed in reference to Fig. 6.

At +160 mV (Fig. 6 A), inactivation is fast and appears nearly complete in 45 ms, while steady state outward current is suppressed by 10 mM internal K^+ (compare Fig. 3, A and B). Superimposed ramp currents obtained from these traces are plotted against time in Fig. 6 A, and against ramp potential in Fig. 6 B. Note that the −40-mV maximum current for the 5-ms test pulse is here quantitatively identical to maximum current for the 5-ms trace in Fig. 5 B. However, this current becomes progressively reduced, while E_{rev} shifts markedly to the right, as slow inactivation develops at the longer test-pulse durations. After a 5-ms test pulse, E_{rev} is −92 mV, shifting to −82 mV after 15 ms. E_{rev} then shifts further to −50 mV after 45 ms, and to −17 mV after 600 ms. Thus, the patch appears to be strongly K^+ selective at −92 mV after a 5-ms pulse, where P_K/P_{Na} is >400. By contrast, after a 600-ms pulse, E_{rev} moves far in the direction of the 0-mV reversal potential predicted for symmetric Na^+ solutions and P_K/P_{Na} falls to 11, demonstrating the relative increase in P_{Na} that coincides with the development of slow inactivation. Note that E_{rev} shifts to the right in Fig. 6 A, coincident with a reduction in peak tail current magnitude, indicating that this shift results from inactivation rather than accumulation of extracellular K^+ ions (as in Fig. 5 A).

It may seem surprising that E_{rev} does not reach zero after the 600-ms pulse in these solutions with symmetrical internal and external Na^+ concentrations, since slow inactivation might be expected to be fully equilibrated by this time. However, we find that peak outward currents are reduced at least 50-fold by this Na^+_i plus K^+_i internal solution, while outward Na^+ currents through inactivated channels are reduced at least 10-fold by the internal K^+ ions. Additionally, even though internal Na^+ ions also block outward K^+ currents, this block is smaller at negative potentials. Thus, the P_K of a noninactivated *Shaker* channel could be as much as two orders of magnitude greater than the P_{Na} of a slow inactivated *Shaker* channel in these solutions. Thus, even where slow inactivated states are strongly absorbing, a small number of noninactivated channels at negative potentials make a disproportionate contribution to the overall P_K/P_{Na} ratio.

The ramp I-V data of Figs. 5 and 6 clarify that N-shaped I-V curves are fully developed after the 5-ms test pulse, before any substantial slow inactivation has occurred. As slow inactivation develops in longer test pulses, these curves show reduced K^+ permeation associated with a marked reduction in the maximum cur-

rent at −40 mV. These effects appear after test pulses to both +40 and +160 mV (although at very different rates), and appear irreversible within the time course of any given ramp. By contrast, the phenomena that underlie the N-shaped I-V curve are apparently instantaneous since the changes in outward current magnitude can be accurately regenerated, without noticeable hysteresis, during the course of a 1-ms ramp.

We conclude that changes in slow inactivation rate cannot be the cause of the N-shaped I-V curve. Rather, it appears that changes in both slow inactivation rate and I-V waveform may result from voltage-dependent changes in the permeation properties of noninactivated channels. Furthermore, the quantitative equivalence of the 5-ms ramps in Figs. 5 and 6 indicate that the initial conditions at +40 and +160 mV are not sufficiently different to affect ramp waveforms. There is, therefore, no evidence to support differences in $[K^+]_i$ as making significant contributions to the initial conditions faced by *Shaker* channels at these two potentials. By contrast, at +40 mV, we see increasing tail current peaks suggestive of accumulation of $[K^+]_o$, whereas no such change in tail current peaks appears after pulses to +160 mV. This evidence additionally supports the primary hypothesis presented here, that P_K falls relative to P_{Na} at positive potentials.

Ramp I-V Curves in Noninactivated Channels: Effects of Changing Ion Concentrations

In this section, we address whether different components of the ramp I-V curve are differentially affected by varying internal and external K^+ concentrations. Our results support the general conclusion that Na^+ permeation increases at positive potentials. When 115 mM Na^+_i competes against 10 mM K^+_i, the currents behave as if they are carried primarily by K^+ ions at negative potentials, but by Na^+ ions at potentials greater than +100 mV. However, we would presume that K^+ ions become increasingly effective competitors even at positive potentials as $[K^+]_i$ is increased beyond 10 mM and $[Na^+]_i$ is reduced, although this point is not addressed in the experiments presented here.

We recognize that changes $[K^+]_i$ and $[K^+]_o$ will affect ramp I-V curves, in part through changes in K^+ driving force. Thus, it might be expected that these data should be replotted as G-V curves to eliminate such driving force effects. Even where the relative contributions of Na^+ and K^+ ions to the observed currents are not clear, each I-V curve indicates a reversal potential, and G_{total} (i.e., the sum of $G_{Na} + G_K$) could be calculated as $I_{total}/(V - E_{rev})$. Unfortunately, such calculations could be highly misleading if the P_K/P_{Na} ratio and, therefore, the relevant E_{rev} are suspected of changing as functions of test potential.

Changing intracellular K^+ concentrations. The effects of changing internal K^+ concentrations are examined in Fig. 7 A, using 5-ms test pulses where ramp I-V curves report the behavior of noninactivated channels. Note that $[K^+]_i$ is indicated for each of the traces in Fig. 7 A and that all traces were obtained from the same inside-out patch. When $[K^+]_i$ is varied in the presence of constant 115 mM $[Na^+]_i$ and $[Na^+]_o$, outward current at negative potentials is eliminated by reducing $[K^+]_i$ to zero. When $[K^+]_i$ is increased to 5 mM, the reversal potential shifts to −60 mV, yielding a P_K/P_{Na} ratio of ∼220 using the Goldman-Hodgkin-Katz (GHK)[1] formalism. Outward K^+ currents are small at negative potentials, as would be expected from previous data describing Na^+ block of these currents (Chandler and Meves, 1965; Bezanilla and Armstrong, 1972; French and Wells, 1977; Begenisich and Cahalan, 1980). At positive potentials, outward currents in the presence of 5 mM internal K^+ are reduced by comparison with outward Na^+ currents in the absence of internal K^+. Apparently, at this low $[K^+]_i$, K^+ block of outward Na^+ currents exceeds any contribution from K^+ efflux to total outward current. A further increase of $[K^+]_i$ to 10 mM markedly increases outward K^+ current at negative potentials, while further left shifting E_{rev} to −93 mV (yielding a calculated P_K/P_{Na} of >400). Nevertheless, total outward current at positive potentials still does not increase above the level of the outward Na^+ currents seen in zero $[K^+]_i$. Thus, at the low internal K^+ concentrations used here, it seems clear that Na^+ ions remain the primary carrier of outward currents at greater than +80 mV.

Changing extracellular K^+ concentrations. Fig. 7 B shows a series of ramp traces obtained from the same outside-out patch. Here the K^+ concentrations indicated in the figure refer to $[K^+]_o$ values. Thus, the N-shaped I-V curve associated with the 0 K^+ trace was obtained in the same solutions as were used for Figs. 5 and 6. When $[K^+]_o$ is varied against a background of constant internal and external Na^+ concentrations, the findings at negative potentials confirm that currents in this range respond as if they are carried primarily by K^+ ions. At positive potentials, increasing $[K^+]_o$ reduces outward currents at +150 mV and right shifts the K^+ current peak by about +60 mV (from −40 mV in 0 mM $[K^+]_o$ to +20 mV in 10 mM $[K^+]_o$). Again, however, the marked effects of changing $[K^+]_o$ on inward currents contrast with the relatively small effects of $[K^+]_o$ on outward currents.

Effects of ion concentrations on reversal potentials. Although reversal potentials measured in ramp I-V curves may be distorted when large outward currents cause K^+ ion accumulation in the pipette, reversal potentials in 115 Na^+_o // 115 Na^+_i + 10 K^+_i solutions range from −85 to −105 mV, indicating a strongly K^+-selective channel at these very

[1]*Abbreviation used in this paper:* GHK, Goldman-Hodgkin-Katz.

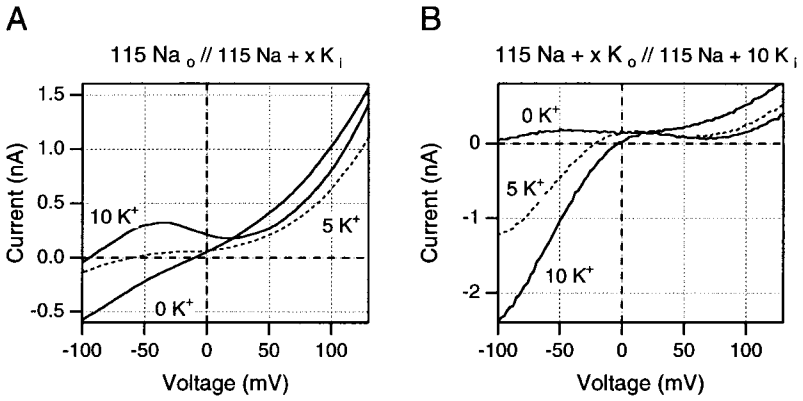

Figure 7. Effects of changes in K^+ concentrations on ramp I-V curves after 5-ms test pulses to +160 mV (A) or +140 mV (B). (A) Effects of changes in internal K^+ concentration in one inside-out patch. Note that the outward currents at positive potentials are highest in absence of internal K^+ and fall when low K^+ concentrations are added to the internal solution. (B) Effects of changes in external K^+ in one outside-out patch. Changes in outward currents are small relative to the changes in inward currents at negative potentials. See text for full discussion of these results. Data in A are from one inside-out patch, data in B are from one outside-out patch.

negative potentials. However, reduction of internal K^+ (Fig. 7 A) from 10 to 5 mM shifts E_{rev} to −50 mV, rather than to approximately −75 mV, as would have been expected if P_K/P_{Na} had remained unchanged.

Permeability ratios were calculated (data not shown) from a range of positive reversal potentials using outside-out patches and symmetrical Na^+ solutions with 2.5, 5, or 10 mM K^+ added only to the external solution. These solutions yielded reversal potentials of +18.3 ± 2.9, +34.7 ± 4.0, and +47.7 ± 6.8 mV, respectively, for three patches exposed to each solution. These reversal potentials imply a marked change away from the K^+-selective behavior expected for a *Shaker* channel.

Ramp I-V Curves in Slow Inactivated Channels

In contrast to the complex results described above, slow inactivated *Shaker* channels appear effectively impermeant to K^+ ions at all potentials, although they retain partial Na^+ permeability. Thus, the ramp I-V curve for slow inactivated channels shown in Fig. 6 B is remarkably linear with no significant deviation at either positive or negative potentials. Apparently, there is little increase in P_{Na} even at very positive potentials in these slow inactivated channels, although it remains possible that such an effect does occur but is balanced by an increasingly effective K^+ block of outward Na^+ currents at more than +80 mV.

Is the N-Shaped I-V Caused by a Conformational Change?

The results presented above indicate that the N-shaped I-V curve results from changes in the relative K^+ and Na^+ permeabilities of noninactivated *Shaker* channels. Recent work by Immke et al. (1999) has shown that the Kv2.1 pore undergoes structural changes in the absence of K^+ ions at some critical site within the selectivity filter. This work raises the possibility that effective Na^+ block of outward K^+ currents at positive potentials might precipitate a structural change that would favor subsequent Na^+ permeation. If such a mechanism occurs here, involving transitions between discrete conformational states of the selectivity filter, then such transitions must be fast compared with the time course of a 1-ms ramp.

Alternatively, voltage-dependent changes in relative permeabilities may result from the inherently constant properties of a single conformational state. This possibility will be evaluated further in the discussion.

DISCUSSION

The present study was undertaken to address the mechanism by which internal and external solutions induce voltage-sensitive slow inactivation rates. Since Starkus et al. (1997) had noted the marked difference in slow inactivation rates associated with outward K^+ currents versus outward Na^+ currents, we concentrated here on solutions containing these two ion species, either separately or together.

The principal results of this study demonstrate several things. (a) Slow inactivation rates in *Shaker* channels remain voltage insensitive under conditions in which there is no significant competition for permeation between K^+ and Na^+ ions (see Fig. 1, A and B). Thus, in $Na^+_o//K^+_i$ solutions, or in $Na^+_o//Na^+_i$ and $K^+_o//K^+_i$ solutions, or with $Tris^+$ externally and either ion internally, slow inactivation remains voltage insensitive. (b) Even where internal solutions are used that contain both Na^+ and K^+ ions, slow inactivation rates do not show significant voltage sensitivity at "physiological" potentials (i.e., at test potentials less than +50 mV; see Fig. 2 A, a and b). In this voltage range, the principal effect of increased $[Na^+]_i$ is to reduce outward K^+ currents, as has been shown for delayed rectifiers (Chandler and Meves, 1965; Bezanilla and Armstrong, 1972; French and Wells, 1977; Begenisich and Cahalan, 1980). Similarly, at these potentials, high $[K^+]_i$ effectively blocks inward Na^+ currents (Korn and Ikeda, 1995; Starkus et al., 1997; Kiss et al., 1998). (c) For internal solutions containing both Na^+ and K^+ ions, slow inactivation rates become markedly voltage sensitive at potentials greater than +50 mV, as if the ion species responsible for the observed outward currents shifts from K^+ at

physiological potentials to Na^+ at very positive potentials (see Fig. 1 D). (d) The waveform of the N-shaped I-V curve appears correlated with the changes in slow inactivation rates (Fig. 2), suggesting that the region of negative slope conductance results from a decrease in outward K^+ currents coincident with increased Na^+ permeation (Fig. 7). (e) These findings imply that Na^+ ions become increasingly capable of permeating *Shaker* channels at more positive potentials, that increased Na^+ permeation is associated with reduced permeation by K^+ ions, and that these changes combine to produce both the N-shaped I-V curve and the voltage sensitivity of slow inactivation. (f) Although the mechanisms responsible for the voltage-dependent changes in relative permeabilities are not defined by this study, some mechanisms can now be either ruled out or strictly limited. First, slow inactivation–induced changes in relative Na^+ and K^+ permeabilities are not the mechanism responsible for the N-shaped I-V curve (see Figs. 5 and 6). Second, the N-shaped curve is not a result of large outward currents at positive potentials causing progressive depletion of internal K^+ ions and so permitting increased Na^+ permeation at positive potentials (Fig. 4 B). Third, if the observed changes in relative permeabilities result from conformational changes in the selectivity filter (compare Immke et al., 1999), then such changes must occur in the microsecond time domain and would need to be 10–100-fold faster than the conformational changes of channel activation and deactivation gating.

That permeant ion species can be profoundly important in determining slow inactivation rates has been noted by López-Barneo et al. (1993), as well as by Baukrowitz and Yellen (1995), Starkus et al. (1997, 1998), Kiss and Korn (1998), and Ogielska and Aldrich (1999). A principal concept developed through this series of papers is that a regulatory site exists towards the outer end of the selectivity filter at which permeant ions have differing efficacies in delaying entry into slow inactivated states, a process that otherwise occurs in a voltage-insensitive manner after channel opening. Since this regulatory site lies near the outer end of the permeation pathway, it can be loaded either directly from the external medium or indirectly from the internal medium during outward currents. Furthermore, the affinity of this regulatory site for K^+ ions is an important determinant of both slow inactivation rates and recovery rates (Ogielska and Aldrich, 1999), although access to this site may also be affected by even conservative mutations in other regions of the selectivity filter.

The conclusions reached here fit well into such a general model, except that previous work has provided little reason to suppose that noninactivated *Shaker* K^+ channels might become relatively Na^+ selective at very positive potentials (but see Immke et al., 1999). Nevertheless, delayed rectifier channels studied by French and Wells (1977) generate N-shaped peak-current I-V curves when exposed to high internal Na^+ and low internal K^+ concentrations. Two alternative interpretations have been provided for the increasing outward currents at positive potentials. French and Wells (1977) suggested that these currents might be carried largely by Na^+ ions as a result of a voltage-dependent change in channel selectivity. Alternatively, Begenisich and Cahalan (1980) showed that such results could be predicted by a 3B2S Eyring model in which voltage-dependent block by internal Na^+ ions was overcome to yield increased K^+ permeation at very positive potentials. To our knowledge, however, this conflict in interpretations has not been resolved by subsequent experimental studies.

The present study provides a substantial amount of direct evidence linking changes in inactivation rate with the changes in slope of the N-shaped I-V curve. And this is complemented by indirect evidence suggesting that the changes in inactivation rate are related to changes in relative permeation by Na^+ and K^+ ions. We show that slow inactivation is voltage insensitive in simple solutions containing only one permeant ion on each side of the membrane. However, slow inactivation becomes voltage sensitive when predicted differences in the contributions of Na^+ and K^+ ions to outward currents might be approximately compensated by their relative concentrations. In other words, where competition for permeation might be expected to be maximal. Under these conditions, K^+ ions gain the advantage at negative potentials, whereas Na^+ ions seem to become the primary permeators at very positive potentials.

The ionic determinants of the N-shaped I-V curve should be addressable experimentally through evaluating the effects of different ionic solutions on ramp I-V waveforms. Fig. 7 A shows a simple, though nonlinear, I-V curve in $Na^+_o//Na^+_i$ solution and evaluates the effects of addition of internal K^+ ions. Outward currents at negative potentials appear in 5 mM K^+ and become well developed when $[K^+]_i$ is increased to 10 mM. By contrast, outward currents at more than +50 mV are reduced rather than increased by these low internal K^+ concentrations. Similarly, Fig. 7 B shows that increasing external K^+ concentration generates large inward currents at negative potentials while decreasing outward currents at positive potentials. These results seem to confirm the hypothesis that *Shaker* channels become relatively Na^+ permeable at very positive potentials, although the resulting outward Na^+ currents can be reduced by competition from K^+ ions. This conclusion is consistent with the finding that slow inactivation time constants at +160 mV were statistically indistinguishable when measured in $Na^+_o//Na^+_i$ solution, or after the addition of 10 mM K^+ to the internal medium (see also Fig. 1 D). Thus, the sum of our experimental evidence supports the interpretation that P_K/P_{Na} contin-

ues to change in favor of increased Na^+ permeation at potentials greater than +50 mV.

Put simply, voltage-dependent Na^+ block of outward K^+ currents seems likely to involve entry of Na^+ ions as far as some blocking site within the transmembrane field. Once this site is reached, a blocking ion could exit by travelling back against the applied field; alternatively, a Na^+ ion can pass through the channel down the applied field, to exit on the outer side of the membrane. The more positive the applied potential, the more Na^+ ions cross the membrane and the greater the outward Na^+ current. If the probability of entry into the high field-strength region of the channel is controlled by ion-selective "filters" with voltage-dependent properties, then such a system should show the overall behavior seen here. What is not yet clear is whether the apparent voltage sensitivity of the filters results from a rapid voltage-dependent conformational change, or whether this might result from the direct effects of voltage on a continuously variable filter. This second possibility is discussed below.

The Voltage Dependence of the P_K/P_{Na} Ratio

Selectivity is usually determined from reversal potentials measured under biionic conditions, following an approach derived from GHK equations (see Hille, 1992). In Fig. 6, we have seen that reversal potentials shift to the right from $\sim E_K$ towards E_{Na} as increasing numbers of channels enter into slow inactivated conformational states (specifically here, the P-type state as defined by Loots and Isacoff, 1998). Clearly, the GHK equations continue to provide useful insights in simple situations of this kind, although their derivation assumes independence of ion fluxes. However, Hodgkin and Keynes (1955) established that K^+ channels show "long pore" properties, and an extensive literature has since confirmed deviations from the independence principle in these channels. Furthermore, voltage-sensitive competition between different ion species occurs in these channels (see Block and Jones, 1997). In effect, the selectivity determined from biionic reversal potentials in K^+ channels indicates the relative permeabilities that result from the sum of all interactions occurring between the two chosen ions and the channel structure. It is, therefore, to be expected that permeability ratios measured for multi-ion pores may vary depending not only on the ionic conditions but also on the membrane potential at which the measurement was made. Thus, our ramp I-V curves suggest that P_K/P_{Na} falls steeply at positive potentials (in constant ionic conditions).

The challenging nature of our principal conclusion, that relative permeabilities for Na^+ and K^+ ions in *Shaker* potassium channels may change substantially as a function of applied voltage, stimulated a search for simple models that could address the potential reasonability of this concept. One possibility would be a voltage-dependent conformational transition by which the selectivity filter would change from a primary, K^+-selective, conformation favored at negative potentials to an alternative conformation, permitting increased Na^+ permeation, at positive potentials. Our present data cannot rule out that model, although they suggest that such transitions, if present, must be very rapid.

On the other hand, interactions occurring between a permeating ion and the channel wall may be sufficient, by themselves, to produce voltage-dependent changes in apparent selectivity. Despite the appeal of the Poisson-Nernst-Planck model used by Nonner et al. (1998) to describe anomalous mole fraction behavior in calcium channels, we chose here to explore this possibility using the simplest possible version of the most widely used permeation model. As shown in Fig. 8, a single binding-site (2B1S) Eyring model proves capable of approximating the N-shaped I-V curves seen in this study.

Models for ion permeation based on Eyring kinetic formulations must be carefully constrained if they are to generate constant permeability ratios across the experimental voltage range and conform to GHK equations (see Hille, 1992). Unless such constraints are applied, even the simplest barrier model (2B1S) may produce voltage-dependent changes in permeability ratios such that the simulated channel, as here, appears K^+ selective at negative potentials and Na^+ selective at more than +60 mV. Fig. 8 shows one such model, which has been adjusted to approximate the I-V data from Fig. 7 A. Model parameters are shown in the figure legend, simulated data traces are plotted in Fig. 8 B, while Fig. 8 C demonstrates the predicted ion fluxes for the same conditions as were used for the 10 K^+ curve shown in Fig. 7 A (as well as for Figs. 1 C, 2, 5, and 6). Fig. 8, B and C, show that reversal potential is −95 mV, where net Na^+ influx is equal to net K^+ efflux. At less negative potentials, outward current increases to a maximum at about −40 mV, and this maximum is clearly dependent on $[K^+]_i$, as in our data (see Fig. 7, A and B). In this model (see Fig. 8 B) it is clear that this outward current is carried primarily by K^+ ions. However, K^+ efflux is progressively reduced at more positive potentials, while Na^+ efflux increases to become larger than K^+ efflux positive to the "saddle" region of the N-shaped I-V curve. Fig. 8 D (open symbols) shows the simulated P_K/P_{Na} ratios obtained from reversal potential measurements in differing ionic solutions, using this model. The voltage-dependent changes in P_K/P_{Na} ratio are similar to the calculated values (filled symbols) obtained in the present study from E_{rev} measurements in the range −100 to +50 mV.

When this model is modified by lowering the height of the external barrier for Na^+ ions, Na^+ block of K^+ efflux at positive potentials is decreased (not shown),

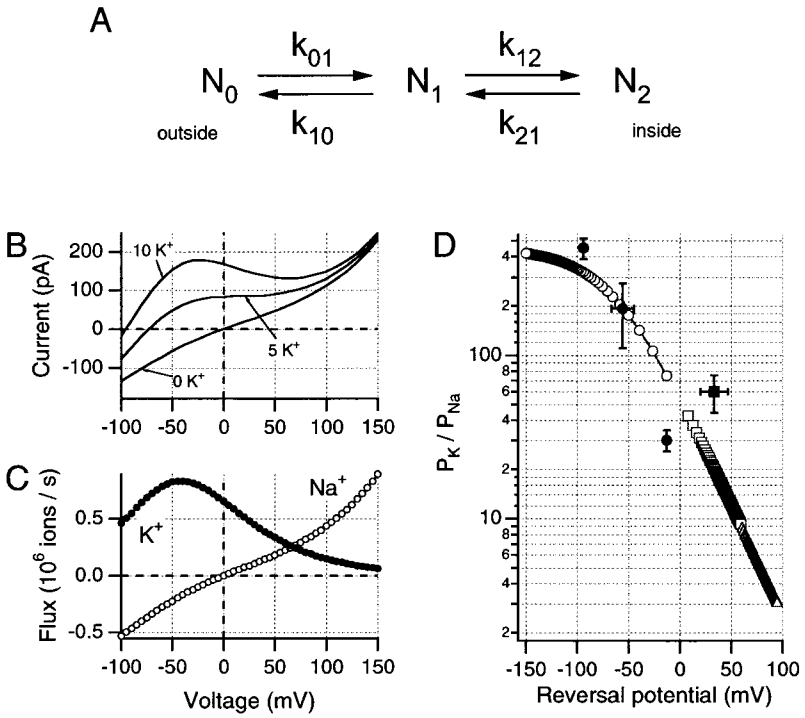

Figure 8. A simple single-site Eyring barrier model can be used to demonstrate voltage-dependent changes in P_K/P_{Na} ratio. Parameters of the model used here can be described in relation to a simple kinetic scheme (A) in which N_0, N_1, and N_2 represent the external, intramembrane, and internal energy wells, respectively; where k_{01} and k_{10} are the forward and backward rate constants between N_0 and N_1, and k_{12} and k_{21} are the equivalent rate constants between N_1 and N_2. Values for these rate constants are shown given for both Na^+ and K^+ ions at 0 mV and the solutions used for the data in Fig. 7 A. Rate constants (s^{-1}): (Na^+) k_{01}, $2.77 \times 10^{+8}$; k_{10}, $1.13 \times 10^{+5}$; k_{12}, $2.05 \times 10^{+8}$; k_{21}, $5.01 \times 10^{+11}$; (K^+) k_{01}, $1.84 \times 10^{+11}$; k_{10}, $4.57 \times 10^{+8}$; k_{12}, $6.18 \times 10^{+7}$; k_{21}, $2.49 \times 10^{+11}$. To calculate the rate constants at other potentials, it is necessary to define the placements of the barriers and wells within the transmembrane field. For the model used here, N_0 and N_2 were presumed to be at 0 and 100% of the electrical distance from the external side of the membrane, while N_1 was set at 45% of this distance. Internal and external energy barriers were placed at 10 and 90% of the transmembrane field, respectively. (B) Simulations of changes in internal K^+ concentrations approximate the data shown in Fig. 7 A, when the same internal and external solutions are used. For this simulation, the patch was presumed to contain 1,500 channels. (C) Predicted single-channel Na^+ and K^+ fluxes were generated by this model for the 10-mM internal K^+ condition, suggesting voltage-dependent changes in relative permeabilities. (D) P_K/P_{Na} ratios obtained from predicted reversal potentials for this model under different ionic conditions. (○) Simulations with 115 Na_o / / 115 Na_i and differing internally, (□) variable external [K^+]. △ were obtained from simulations using internal 11.5 mM Na^+, external 115 mM Na^+, and variable K^+. Experimental values obtained in this study are shown as filled symbols (mean ± SD): ●, Na^+_o / / Na^+_i + variable K^+; ■, Na^+_o + 2.5–10 mM K^+_o / / Na^+_i.

thus increasing the total outward current at these potentials. As pointed out by Begenisich and Cahalan (1980), the N-shaped I-V curve is readily predicted by Eyring models, although, as we see here, such simulations can be equally supportive of the claim first made by French and Wells (1977) that Na^+ may become the primary outward current carrier at more than +100 mV. Thus, the most commonly used approach for modeling channel selectivity predicts that the P_K/P_{Na} ratio can change continuously in a voltage-dependent manner without requiring discontinuous changes in channel properties. We conclude that our observations are not necessarily indicative of a voltage-dependent change in channel structure, but could result, as in the Fig. 8 model, simply from a maintained asymmetry of the internal and external barrier heights faced by the less permeant ion. In this case, it seems arguable that selectivity, an inherent property of channel structure, remains constant despite the observed voltage-dependent changes in relative permeabilities.

In overview, this paper has described a complex interaction between voltage- and state-dependent (i.e., slow inactivation related) changes in relative Na^+ and K^+ permeabilities. We demonstrate that the apparent voltage sensitivity of slow inactivation in outward currents occurs only when two different ion species might be expected to compete for passage via the permeation path to reach a relatively externally located regulatory site controlling slow inactivation rates. Our findings support the interpretation that the P_K/P_{Na} ratio would reach fractional levels at very positive potentials (as suggested by the simulations of Fig. 8 D). At these high potentials, the residency time of K^+ ions at the regulatory site should be much reduced compared with Na^+ ion residencies, and entry into slow inactivated states would be consequently facilitated.

We thank R.S. Eisenberg for many stimulating discussions during the course of this work. Additionally, Karyn Karp and Mark Henteleff provided technical assistance on this project.

J.G. Starkus and M.D. Rayner have been supported in part by National Institutes of Health grant RO1-NS21151 (to J.G. Starkus), as well as by grants from the American Heart Association (Hawaii Affiliate). J.G. Starkus received additional support from Pacific Biomedical Research Center Bridging Funds, and from the Max Planck Society. S.H. Heinemann was supported by the Max Planck Society. M.D. Rayner received additional support from the Queen Emma Foundation.

Submitted: 29 March 1999
Revised: 9 December 1999
Accepted: 10 December 1999
Released online: 17 January 2000

REFERENCES

Basso, C., P. Labarca, E. Stefani, O. Alvarez, and R. Latorre. 1998. Pore accessibility during C-type inactivation in *Shaker* K^+ channels. *FEBS Lett*. 429:375–380.

Baukrowitz, T., and G. Yellen. 1995. Modulation of K^+ current by frequency and external $[K^+]$: a tale of two inactivation mechanisms. *Neuron*. 15:951–960.

Begenisich, T.B., and M.D. Cahalan. 1980. Sodium channel permeation in squid giant axons II: non-independence and current–voltage relations. *J. Physiol*. 307:243–257.

Bezanilla, F., and C.M. Armstrong. 1972. Negative conductance caused by entry of sodium and cesium ions into the potassium channels of squid axons. *J. Gen. Physiol*. 60:588–608.

Block, B.M., and S.W. Jones. 1997. Delayed rectifier current of bullfrog sympathetic neurons: ion–ion competition, asymmetrical block and effects of ions on gating. *J. Physiol*. 499:403–416.

Chandler, W.K., and H. Meves. 1965. Voltage clamp experiments on internally perfused giant axons. *J. Physiol*. 180:788–820.

Doyle, D.A., J.M. Cabral, R.A. Pfuetzner, A. Kuo, J.M. Gulbis, S.L. Cohen, B.T. Chait, and R. MacKinnon. 1998. The structure of the potassium channel: molecular basis of K^+ conduction and selectivity. *Science*. 280:69–77.

French, R.J., and J.B. Wells. 1977. Sodium ions as blocking agents and charge carriers in the potassium channel of the squid giant axon. *J. Gen. Physiol*. 70:707–724.

Hamill, O.P., A. Marty, E. Neher, B. Sakmann, and F.J. Sigworth. 1981. Improved patch-clamp techniques for high-resolution current recording from cells and cell-free membrane patches. *Pflügers Arch*. 391:85–100.

Heinemann, S.H., F. Conti, and W. Stühmer. 1992. Recording of gating currents from *Xenopus* oocytes and gating noise analysis. *Methods Enzymol*. 207:353–368.

Hille, B. 1992. Ion Channels of Excitable Membranes. 2nd Ed. Sinauer Associates, Inc., Sunderland, MA. 607 pp.

Hodgkin, A.L., and R.D. Keynes. 1955. The potassium permeability of a giant nerve fibre. *J. Physiol*. 128:61–88.

Hoshi, T., W.N. Zagotta, and R.W. Aldrich. 1990. Biophysical and molecular mechanisms of *Shaker* potassium channel inactivation. *Science*. 250:533–538.

Hoshi, T., W.N. Zagotta, and R.W. Aldrich. 1991. Two types of inactivation in *Shaker* K^+ channels: effects of alterations in the carboxy-terminal region. *Neuron*. 7:547–556.

Iverson, L.E., and B. Rudy. 1990. The role of divergent amino and carboxyl domains on the inactivation properties of potassium channels derived from the *Shaker* gene of *Drosophila*. *J. Neurosci*. 10:2903–2916.

Immke, D., M. Wood, L. Kiss, and S.J. Korn. 1999. Potassium-dependent changes in the conformation of the Kv2.1 potassium channel pore. *J. Gen. Physiol*. 113:819–836.

Kiss, L., and S.J. Korn. 1998. Modulation of C-type inactivation by K^+ at the potassium channel selectivity filter. *Biophys. J*. 74:1840–1849.

Kiss, L., D. Immke, J. LoTurco, and S.J. Korn. 1998. The interaction of Na^+ and K^+ in a voltage-gated potassium channel. Evidence for cation binding sites of different affinity. *J. Gen. Physiol*. 111: 185–206.

Korn, S.J., and S.R. Ikeda. 1995. Permeation selectivity by competition in a delayed rectifier potassium channel. *Science*. 269:410–412.

Levy, D.L., and C. Deutsch. 1996. Recovery from C-type inactivation is modulated by extracellular potassium. *Biophys. J*. 70:798–805.

Liu, Y., M.E. Jurman, and G. Yellen. 1996. Dynamic rearrangement of the outer mouth of a K^+ channel during gating. *Neuron*. 16: 859–867.

López-Barneo, J., T. Hoshi, S.H. Heinemann, and R.W. Aldrich. 1993. Effects of external cations and mutations in the pore region on C-type inactivation of *Shaker* potassium channels. *Receptors Channels*. 1:61–71.

Loots, E., and E.V. Isacoff. 1998. Protein rearrangements underlying slow inactivation of the *Shaker* K^+ channel. *J. Gen. Physiol*. 112: 377–389.

McCormack, K., W.J. Joiner, and S.H. Heinemann. 1994. A characterization of the activating structural rearrangements in voltage-dependent *Shaker* K^+ channels. *Neuron*. 12:301–315.

Nonner, W., D.P. Chen, and B. Eisenberg. 1998. Anomalous mole fraction effect, electrostatics and binding in ionic channels. *Biophys. J*. 74:2327–2334.

Ogielska, E.M., W.N. Zagotta, Z. Hoshi, S.H. Heinemann, J. Haab, and R.W. Aldrich. 1995. Cooperative subunit interactions on C-type inactivation of K channels. *Biophys. J*. 69:2449–2457.

Ogielska, E.M., and R.W. Aldrich. 1998. A mutation in S6 of *Shaker* potassium channels decreases K^+ affinity of an ion binding site revealing ion–ion interactions in the pore. *J. Gen. Physiol*. 112: 243–257.

Ogielska, E.M., and R.W. Aldrich. 1999. Functional consequences of a decreased potassium affinity in a potassium channel pore. Ion interactions and C-type inactivation. *J. Gen. Physiol*. 113:347–358.

Olcese, R., R. Latorre, L. Toro, F. Bezanilla, and E. Stefani. 1997. Correlation between charge movement and ionic current during slow inactivation in *Shaker* K^+ channels. *J. Gen. Physiol*. 110:579–589.

Panyi, G., Z. Sheng, and C. Deutsch. 1995. C-type inactivation of a voltage-gated K^+ channel occurs by a cooperative mechanism. *Biophys. J*. 69:896–903.

Schlief, T., R. Schönherr, and S.H. Heinemann. 1996. Modification of C-type inactivation *Shaker* potassium channels by chloramine-T. *Pflügers Arch*. 431:483–493.

Starkus, J.G., L. Kuschel, M.D. Rayner, and S.H. Heinemann. 1997. Ion conduction through C-type inactivated *Shaker* channels. *J. Gen. Physiol*. 110:539–550.

Starkus, J.G., L. Kuschel, M.D. Rayner, and S.H. Heinemann. 1998. Macroscopic Na^+ currents in the "nonconducting" *Shaker* potassium channel mutant W434F. *J. Gen. Physiol*. 112:85–93.

Yellen, G., D. Sodickson, T.V. Chen, and M.E. Jurman. 1994. An engineered cysteine in the external mouth of a K^+ channel allows inactivation to be modulated by metal binding. *Biophys. J*. 66: 1068–1075.

Zagotta, W.N., T. Hoshi, and R.W. Aldrich. 1990. Restoration of inactivation in mutants of *Shaker* potassium channels by a peptide derived from ShB. *Science*. 250:568–571.